Modelling methane emissions from wetlands

Shushi Peng
Philippe Ciais, Shilong Piao, Bruno Ringeval

LGGE, LSCE, PKU

Outline

1. Why Methane & Interesting hypotheses

2. Modeling methane emissions from wetlands

3. Challenges

Why Methane?

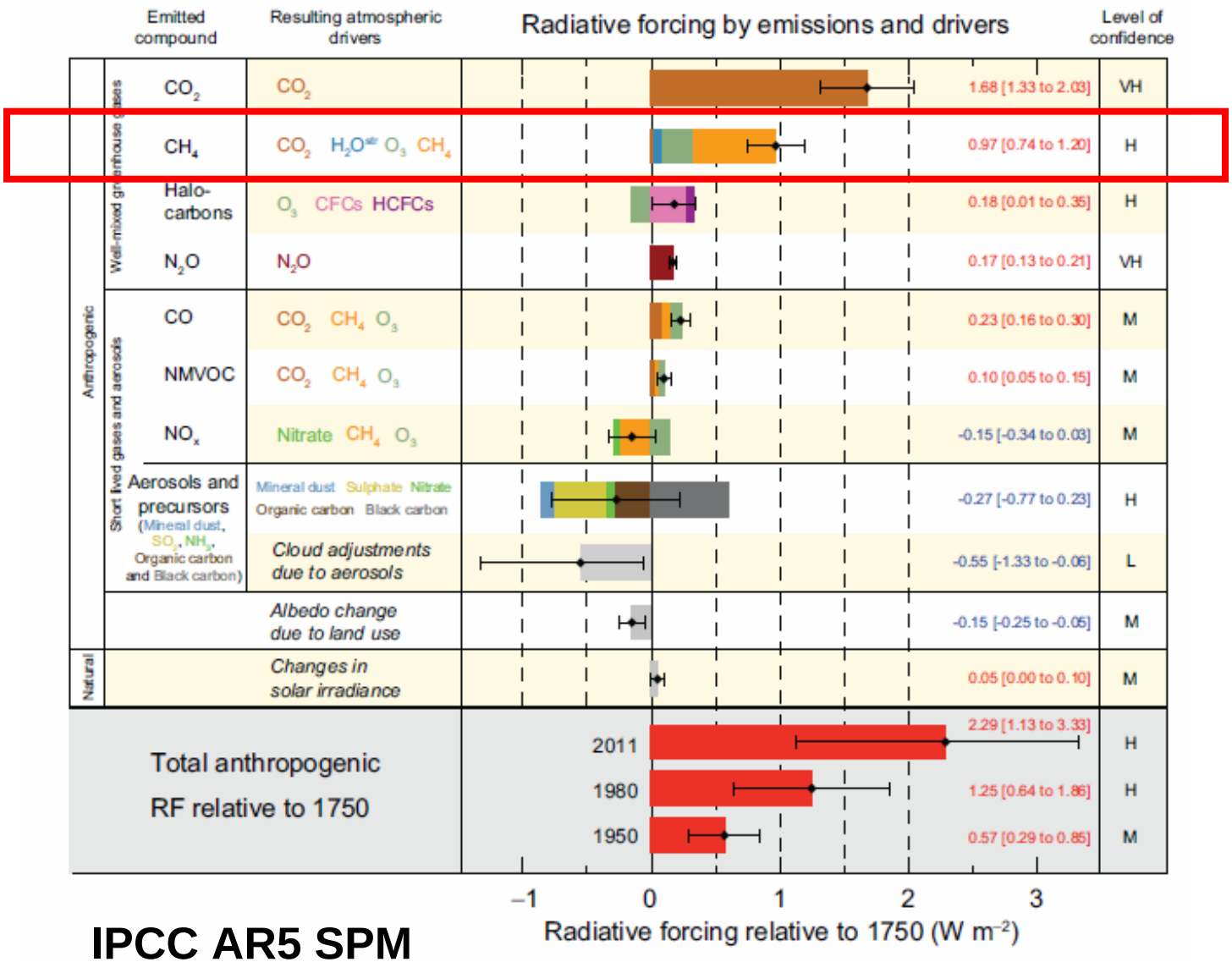

IPCC AR5 SPM

Methane increase, stop then rise again?

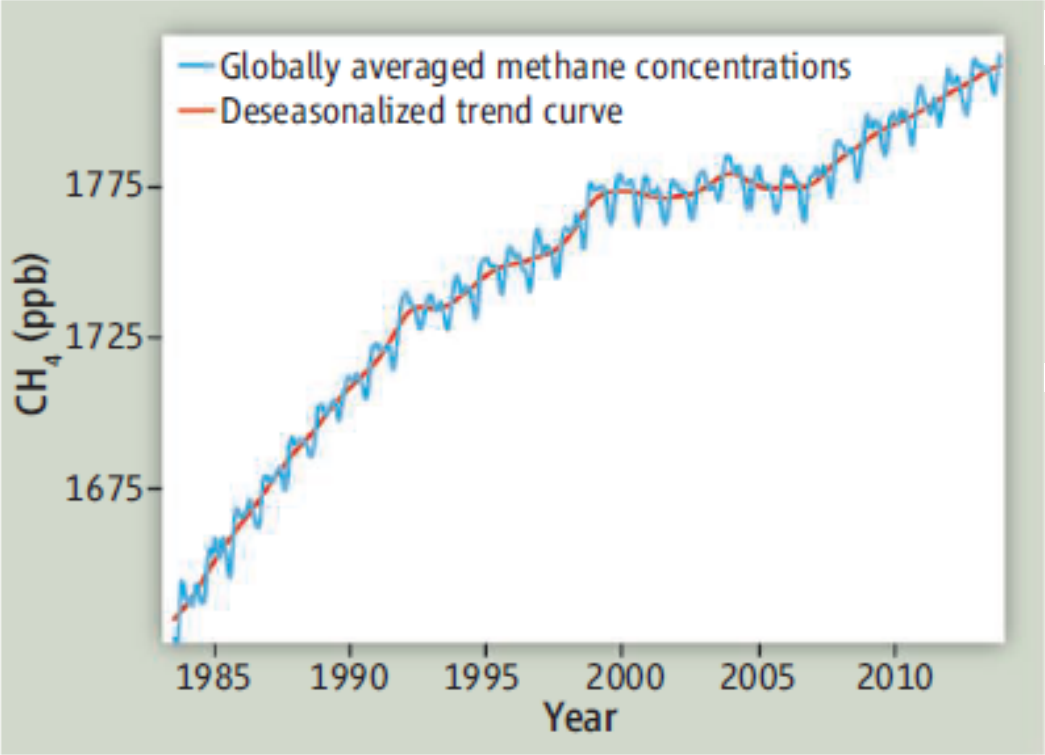

Methane ups and downs. Globally averaged atmospheric methane concentrations rose quickly before 1992. The rise then slowed and almost stopped between 1999 and 2006, but resumed in 2007. Data from ftp://ftp.cmdl.noaa.gov/ccg/ch4/flask/event/.

www.sciencemag.org SCIENCE VOL 343 31 JANUARY 2014

ATMOSPHERIC SCIENCE

Methane on the Rise—Again

Euan G. Nisbet,[1] Edward J. Dlugokencky,[2] Philippe Bousquet[3]

Atmospheric concentrations of the greenhouse gas methane are rising, but the reasons remain incompletely understood.

NATURE | VOL 476 | 11 AUGUST 2011

LETTER

doi:10.1038/nature10259

Reduced methane growth rate explained by decreased Northern Hemisphere microbial sources

Fuu Ming Kai[1]†, Stanley C. Tyler[1]†, James T. Randerson[1] & Donald R. Blake[2]

BRIEF COMMUNICATIONS ARISING

No inter-hemispheric $\delta^{13}CH_4$ trend observed

ARISING FROM Kai, F. M., Tyler, S. C., Randerson, J. T. & Blake, D. R. *Nature* **476**, 194–197 (2011)

nature geoscience

REVIEW ARTICLE

PUBLISHED ONLINE: 22 SEPTEMBER 2013 | DOI: 10.1038/NGEO1955

Three decades of global methane sources and sinks

Stefanie Kirschke *et al.**

Nisbet et al., 2014, Science

Methane increase, stop then rise again?

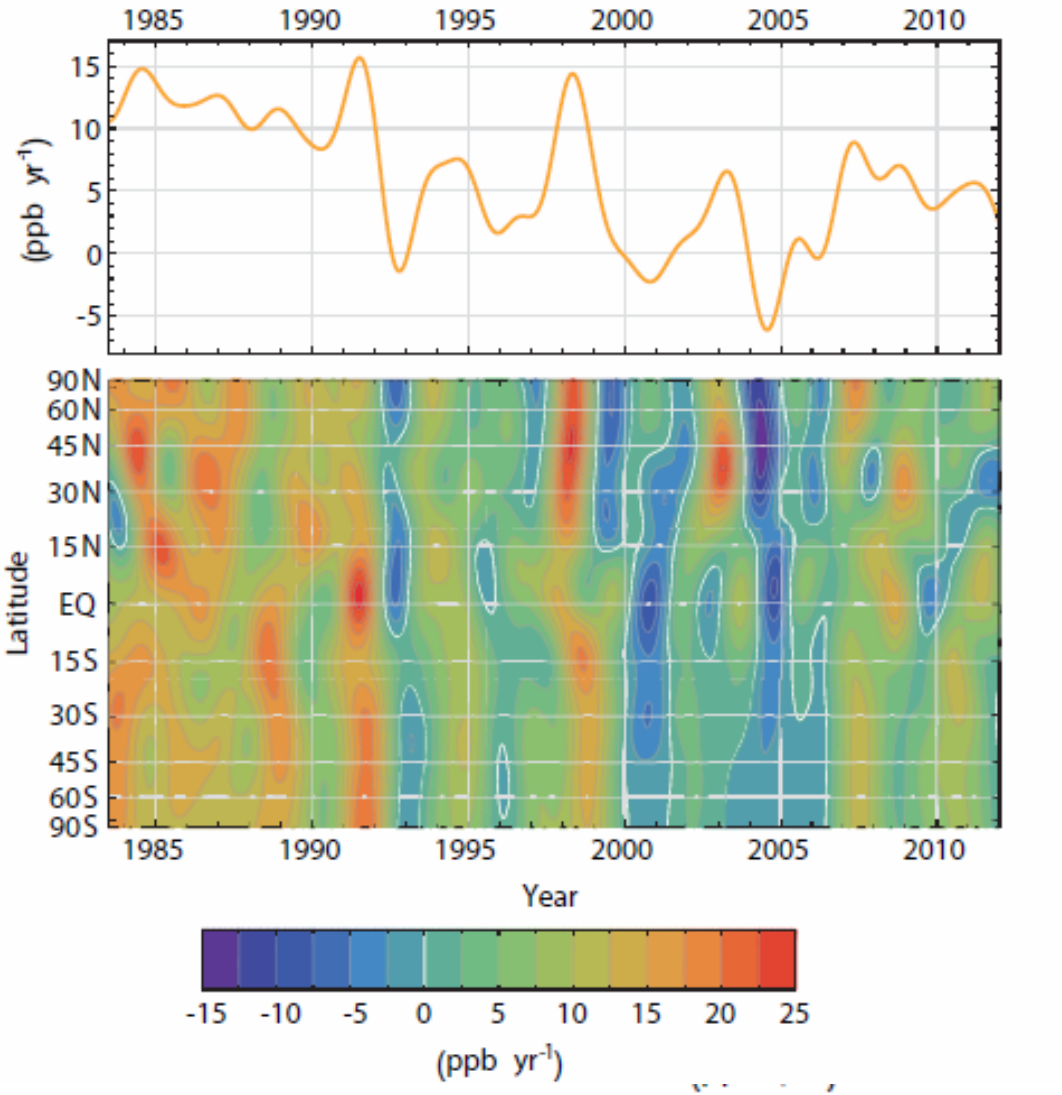

Emissions decrease hypotheses

Fossil fuel decrease?

Rice agriculture decrease?

???

IPCC AR5 Fig 6.18

Figure 6.18 | (Top) Globally averaged growth rate of atmospheric CH_4 in ppb yr^{-1} determined from the National Oceanic and Atmospheric Administration–Earth System Research Laboratory (NOAA–ESRL) network, representative for the marine boundary layer. (Bottom) Atmospheric growth rate of CH_4 as a function of latitude (Masarie and Tans, 1995; Dlugokencky and Tans, 2013b).

Large uncertainty of wetland methane emissions?

Table 1 | CH_4 budget for the past three decades.

	Tg CH_4 yr^{-1}					
	1980–1989		1990–1999		2000–2009	
	Top-down	Bottom-up	Top-down	Bottom-up	Top-down	Bottom-up
Natural sources	203 [150–267]	355 [244–466]	182 [167–197]	336 [230–465]	218 [179–273]	347 [238–484]
Natural wetlands	167 [115–231][19,21,76]	225 [183–266][40,41]	150 [144–160][21,74,77]	206 [169–265][40–42]	175 [142–208][46,53,73,75,77,86]	217 [177–284][40–42]

Figure 2 | Evolution of uncertainty on estimates of methane emissions and sinks presented in Table1. Circle size depicts the robustness of the estimate (number of studies). Circle colour illustrates the level of agreement among studies (min–max ranges): green, high confidence; yellow, medium confidence; red (with black dot), low confidence. Circles are grey when only one study has been used. A large green circle, for example, indicates a very good level of confidence[44].

Kirschke et al., 2013

Vulnerability of the methane budget to paleoclimate?

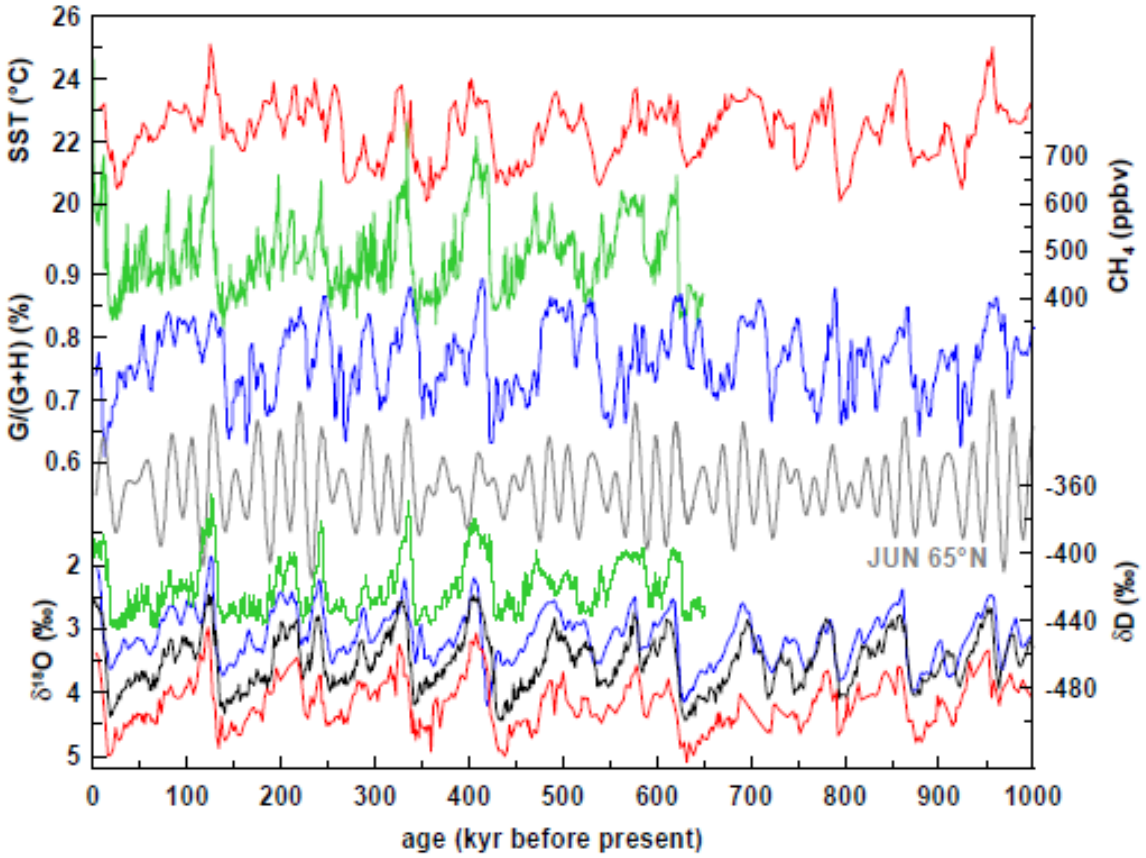

Figure 4.6: Paleoclimate records of the last million years: LR04 δ^{18}O stack (black) [*Lisiecki and Raymo*, 2005], SST and δ^{18}O from marine sediment ODP 846B (red) [*Lawrence et al.*, 2006; *Mix et al.*, 1995], δ^{18}O and goethite (G) & hematite (H) percentages from terrigenous fractions of a sediment in the western tropical Atlantic indicating variations of Amazonian lowland precipitation (blue) [*Harris and Mix*, 1999], EPICA Dome C and Vostok CH_4 and Dome C δD (green, data as in Fig. 4 of *Spahni et al.*, 2005), variation of insolation in June at 65° N on a relative scale (grey) [*Quinn et al.*, 1991]. All data are plotted on individual time scales, that differ during certain stages. This is visible in the δ^{18}O and δD records (bottom curves).

Methane vs. rapid glacial-interglacial climate change ?

Typical isotopic signatures of different methane sources

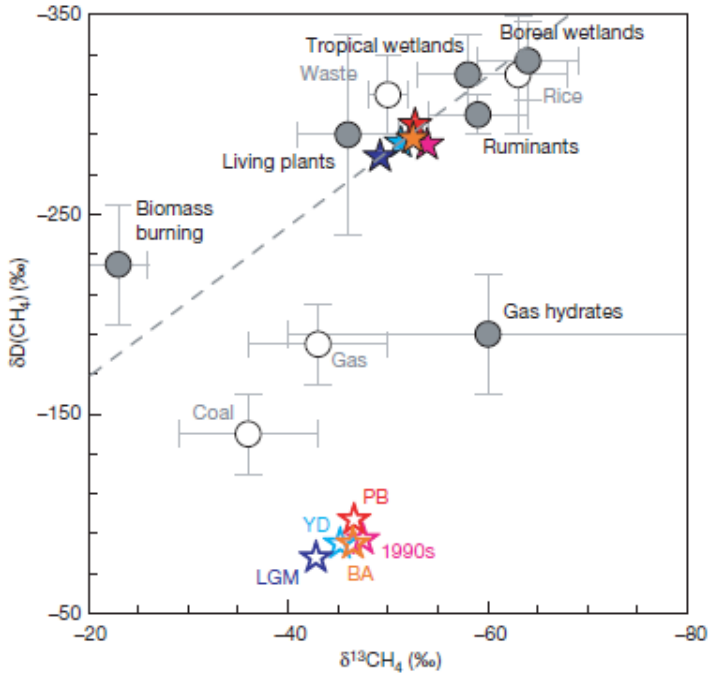

Figure 1 | Typical carbon and hydrogen isotopic signatures of different CH_4 sources used in the Monte Carlo model. Data are from refs 10 and 11 and

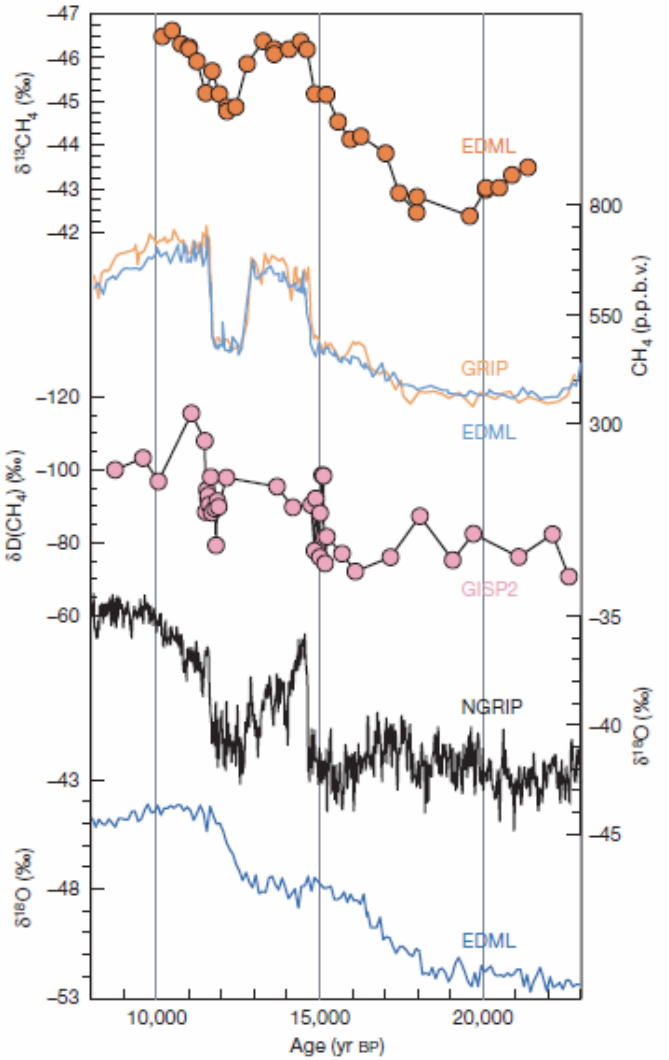

Figure 2 | Glacial/interglacial changes in methane and climate. Carbon

Fisher et al., 2008, Nature

Methane from boreal wetlands during glacial-deglacial transition?

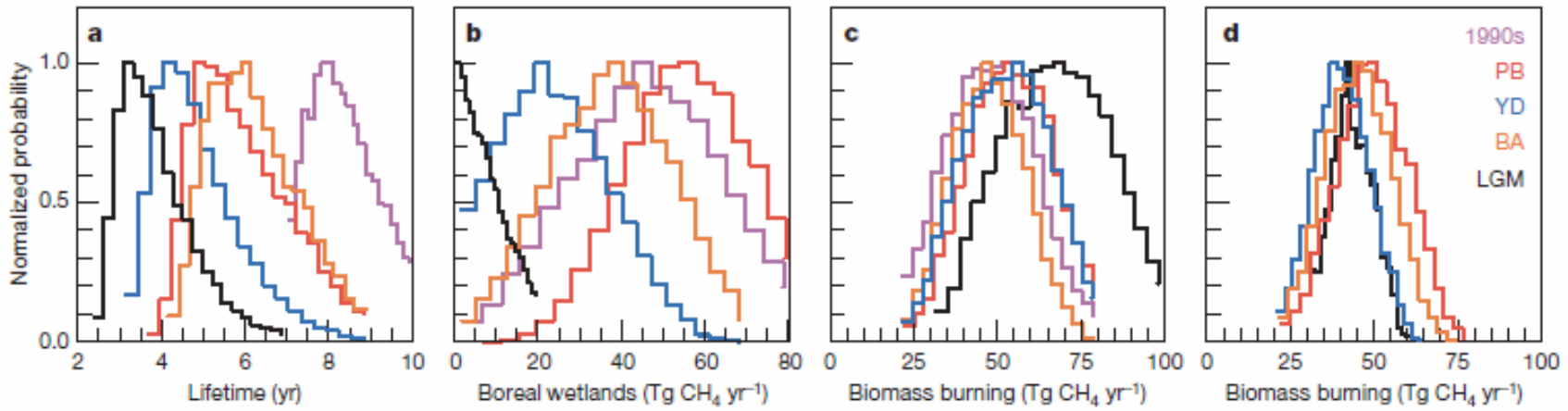

Fisher et al., 2008, Nature

methane is reduced during cold climate periods. We also show that boreal wetlands are an important source of methane during warm events, but their methane emissions are essentially shut down during cold climate conditions.

Methane is possibly the most intriguing and least understood of the naturally occurring atmospheric greenhouse gases. It shows far greater sensitivity and covariance with climate change than carbon dioxide (5), especially with the rapid and transient transitions discovered from the last climatic cycle. It also has been hy-

Behl et al., 2011, PNAS

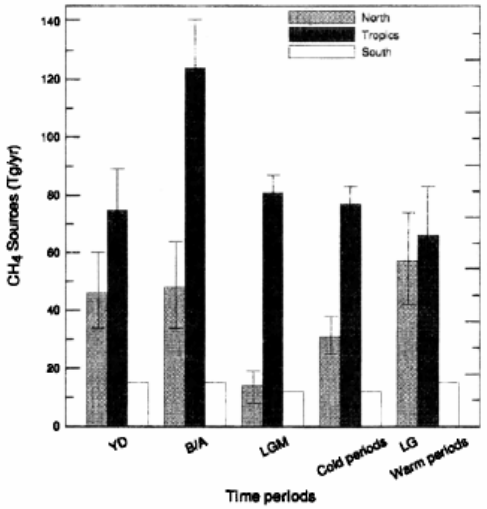

Figure 3. Source distribution among the three boxes of our model for each of the selected time intervals (warm and cold stages during the Last Glacial (LG), the Last Glacial Maximum (LGM), the Bølling/Allerød (B/A) and the Younger Dryas (YD) period). The source in box South was fixed at 12 Tg/yr during the LGM and the cold periods respectively at 15 Tg/yr during the other time intervals.

Dallenbash et al., 2000, GRL

Modeling methane emissions from wetlands

Methane from wetlands

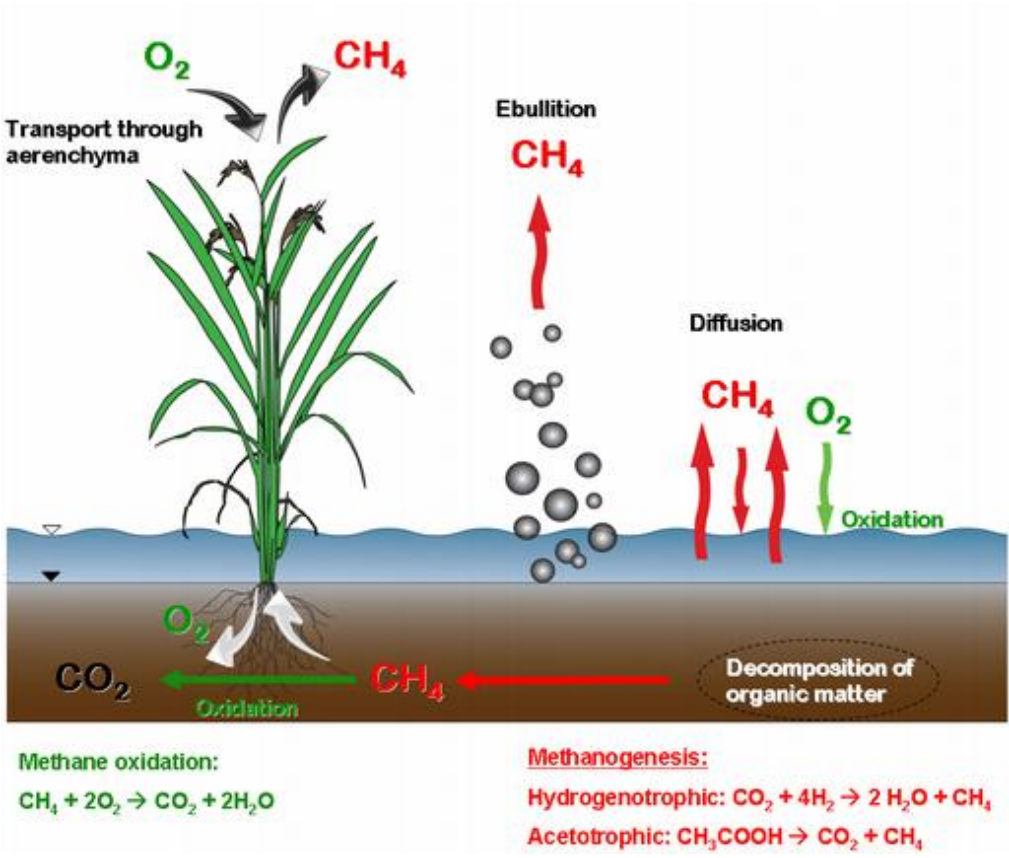

Total methane emission :

Methane production rate * wetland area

www.ibp.ethz.ch

Modeling methane emissions processes

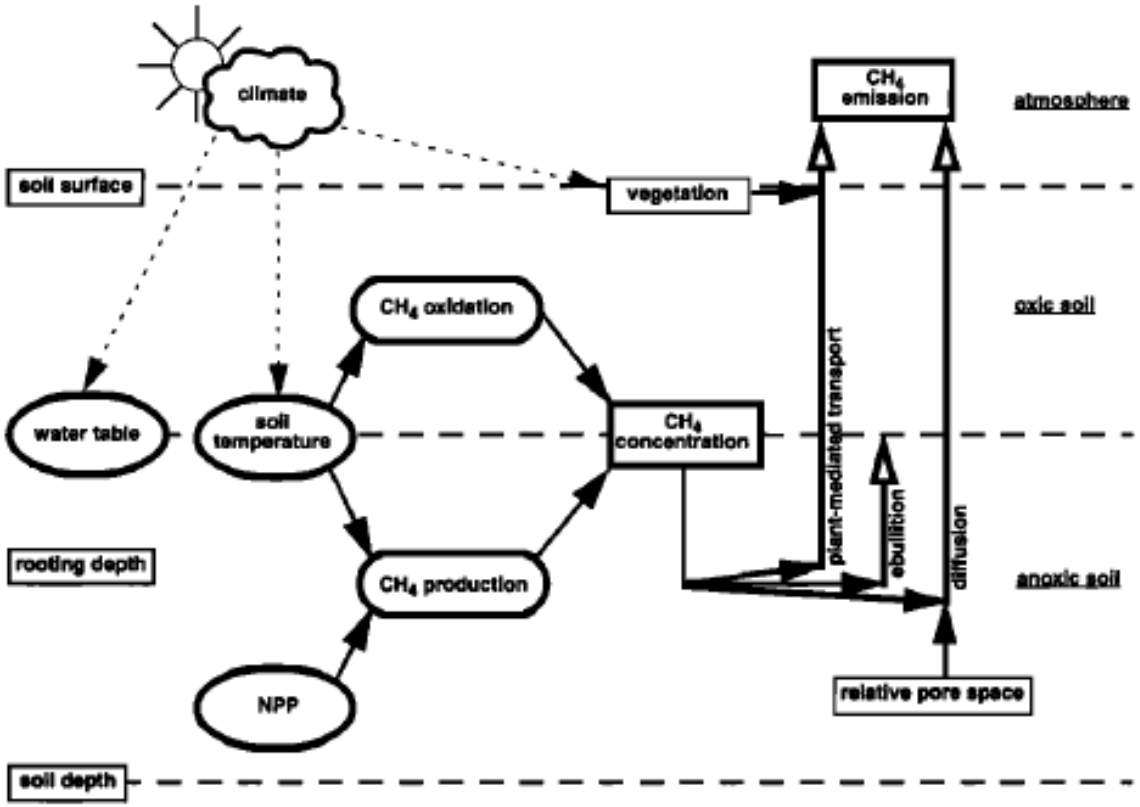

Figure 1. Schematic of the one-dimensional methane model. The processes leading to methane emission to the atmosphere occur in the soil between soil depth and soil surface. Methane production takes place in the anoxic soil below the water table; the methane production rate depends on soil temperature and NPP. Methane oxidation occurs in the oxic soil above the water table and depends on temperature. The model calculates methane concentrations in each (1 cm thick) soil layer. Transport occurs by diffusion through water-/air-filled soil pores, ebullition to the water table, and plant-mediated transport from layers above the rooting depth. Methane emission to the atmosphere is calculated daily.

Walter et al., 2001, JGR

Modeling wetland methane scheme

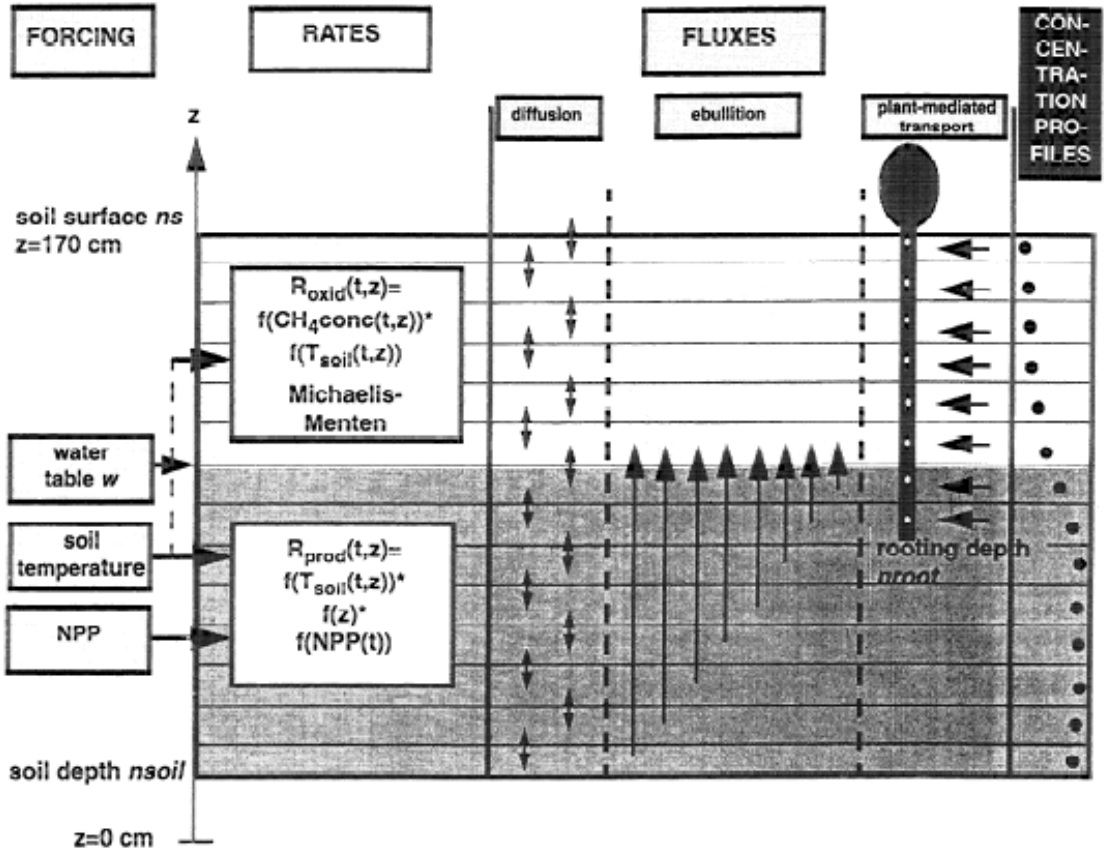

Figure 1. Schematic representation of the model structure. The one-dimensional soil column is divided into 1 cm thick parallel layers. The forcing consists of daily records of the water table, the soil temperature, and the NPP. Methane production occurs in the soil zone between the soil depth nsoil and the water table w, which can be either below or above the soil surface ns. The methane production rate $R_{prod}(t,z)$ is a function of the soil temperature $T_{soil}(t,z)$ and the NPP, which is taken as a measure for substrate availability. Methane oxidation is confined to the soil layers between the water table and the soil surface. The methane oxidation rate $R_{oxid}(t,z)$ follows Michaelis-Menten kinetics and is a function of the soil temperature $T_{soil}(t,z)$. Transport proceeds by (1) molecular diffusion through the soil pores, (2) ebullition, which is the formation of gas bubbles in the water saturated layers and their ascent to the water table, and (3) plant-mediated transport from layers above the rooting depth nroot to the atmosphere. The model calculates methane fluxes to the atmosphere and methane concentration profiles in the soil on a daily basis.

Walter et al., 2000, GBC

Modeling Methane

Take ORCHIDEE as an example:

$$R_{prod}(t,z) = \alpha_0 * f_{org}(z) * C_L(t) * f(T(t,z)) * Q_{10}^{\frac{T(t,z)-T_{mean}}{10}}$$

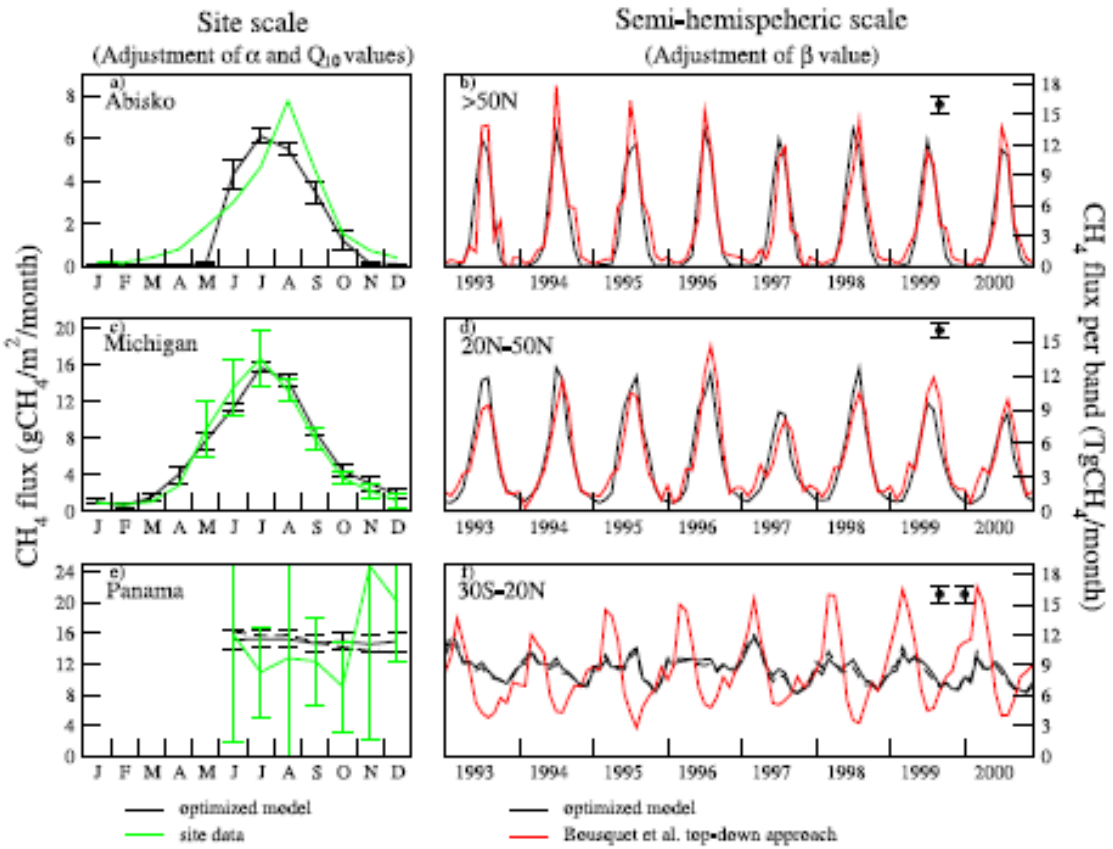

Ringeval et al., 2010, GBC

Methane production rate modeling in ten models?

Table 1. List of WETCHIMP participating models. Not all models contributed results to all experiments. The conceptualized, general description of net methane flux, F, by each model is adapted from Table 5 in Wania et al. (2012). This formulation is for illustrative purposes; thus the main variables and parameters used in CH_4 production are detailed, but oxidation, O, and atmospheric oxidation, O_{atm}, are not. For all results presented in this paper, all O_{atm} values were set to 0, allowing comparison of modelled gross fluxes. All variables listed are described in the table footnotes. Note that identical parameters/variables for different models do not imply identical values used in the models. A full listing of contributed experiments and model set-ups for the experiments, as well as greater detail on the models' methane flux parameterizations, is provided in Wania et al. (2012).

Model	Resolution (long. × lat.)	Coverage	Wetland determination scheme	CH_4 flux parameterization (see table footnotes)**	Principal references
CLM4Me	2.5° × 1.9°	Global	Model-simulated runoff and water table depth used in diagnostic equation that was parameterized for best fit to the GIEMS dataset.	$F = (R_{het} r_{CH4:C} f_{pH} f_{pE} Q_{10} - O) f_{transport} - O_{atm}$	Riley et al. (2011)
DLEM	0.5° × 0.5°	Global	Maximal extents from inundation dataset with simulated intra-annual dynamics.	$F = (P_{max} C_{labile} f_T f_{pH} f_\Theta - O_{trans} - O_{soil}) f_{transport} - O_{atm}$	Tian et al. (2010, 2011); Xu and Tian (2012)
IAP-RAS	0.5° × 0.5°	Global	Prescribed extents from land cover dataset (CDIAC NDP017).	$F = f_T f_\Theta Q_{10}$	Mokhov et al. (2007); Eliseev et al. (2008)
LPJ-Bern	0.5° × 0.5°	Global	Prescribed peatlands and monthly inundation. Simulated dynamic wet mineral soils (saturated, non-inundated).	Peat: $F = (R_{het} r_{CH4:C} f_{root} f_{WTP} - O) f_{transport}$ Wetlands: $F = R_{het} r_{CH4:C}$ Wet soils: $F = R_{het} r_{CH4:C} f_\Theta - O_{atm}$	Spahni et al. (2011)
LPJ-WHyMe	0.5° × 0.5°	Peatlands (> 35° N)	Prescribed peatland extents (Tarnocai et al., 2009) with simulated saturated/unsaturated conditions.	$F = (R_{het} r_{CH4:C} f_{root} f_{WTP} - O) f_{transport}$	Wania et al. (2009a,b, 2010)
LPJ-WSL	0.5° × 0.5°	Global	Prescribed from monthly inundation dataset.	$F = R_{het} r_{CH4:C} f_{ecosys}$	Hodson et al. (2011)
ORCHIDEE	1.0° × 1.0°	Global	Mean yearly extent over 1993–2004 period scaled to that of inundation dataset with model calculated intra- and inter-annual dynamics.	$F = (R_0 C_{labile} f_{WTP} f_T Q_{10} - O) f_{transport}$	Ringeval et al. (2010, 2011) Ringeval (2011) Ringeval et al. (2012)
SDGVM	0.5° × 0.5°	Global	Independently simulated extents.	$F = R_{het} r_{CH4:C} f_{WTP} f_T Q_{10} - O$	Hopcroft et al. (2011)
UVic-ESCM	3.6° × 1.8°	Global	Independently simulated extents.	n.a.	Singarayer et al. (2011) Avis et al. (2011)
UW-VIC	100 km*	W. Siberian lowlands	Prescribed peatland extents with inundation dataset dynamics modulated by internally calculated saturated/unsaturated conditions.	$F = (R_0 f_{NPP} f_{root} f_T Q_{10} - O) f_{transport}$	Bohn et al. (2007); Bohn and Lettenmaier (2010)

* 100 km polar azimuthal equal-area grid (EASE grid), resampled to 0.5° × 0.5°.
** Summary of variable names: C_{labile}: labile carbon pool; O_{soil}: oxidation in the soil pore water; O_{trans}: oxidation associated with transport through plants; P_{max}: maximum CH_4 production; Q_{10}: factor describing dependence on temperature; R_{het}: heterotrophic respiration; R_0: CH_4 production rate; f_{ecosys}: function of ecosystem type; f_{NPP}: function of the ratio of monthly to annual net primary production (NPP); f_{pE}: function of alternative electron acceptors; f_{pH}: function of pH value; f_{root}: function of vertical root distribution; f_T: function of temperature; f_Θ: function of soil moisture; $f_{transport}$: function of CH_4 transport; f_{WTP}: function of water table position; and $r_{CH4:C}$: fraction of C converted to CH_4.

Melton et al., 2013

Modeling wetland area --- TOPMODEL

TOPMODEL

(a) Vogüe catchment in France

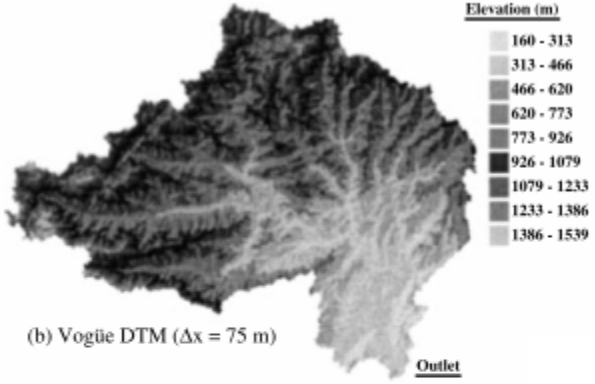

(b) Vogüe DTM (Δx = 75 m)

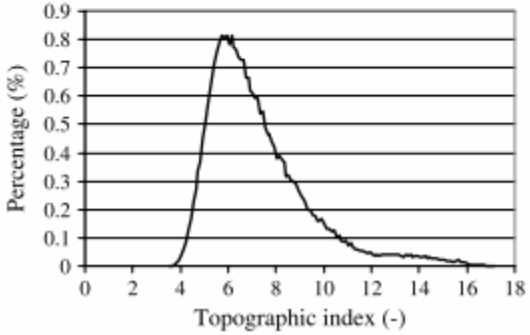

Topographic index

$$\lambda_i = \ln(a_i / \tan\beta_i)$$

One **grid-cell** g: D_t , $\overline{\lambda}$

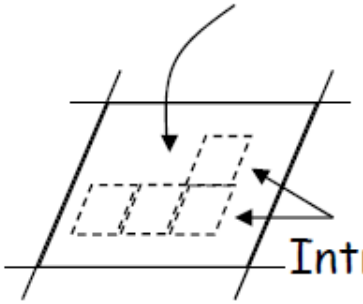

Introduction of a sub-grid scale:

divide g into many **pixels**

$(d_{1,t}, \lambda_1), (d_{2,t}, \lambda_2), \ldots, (d_{i,t}, \lambda_i)$

TOPMODEL

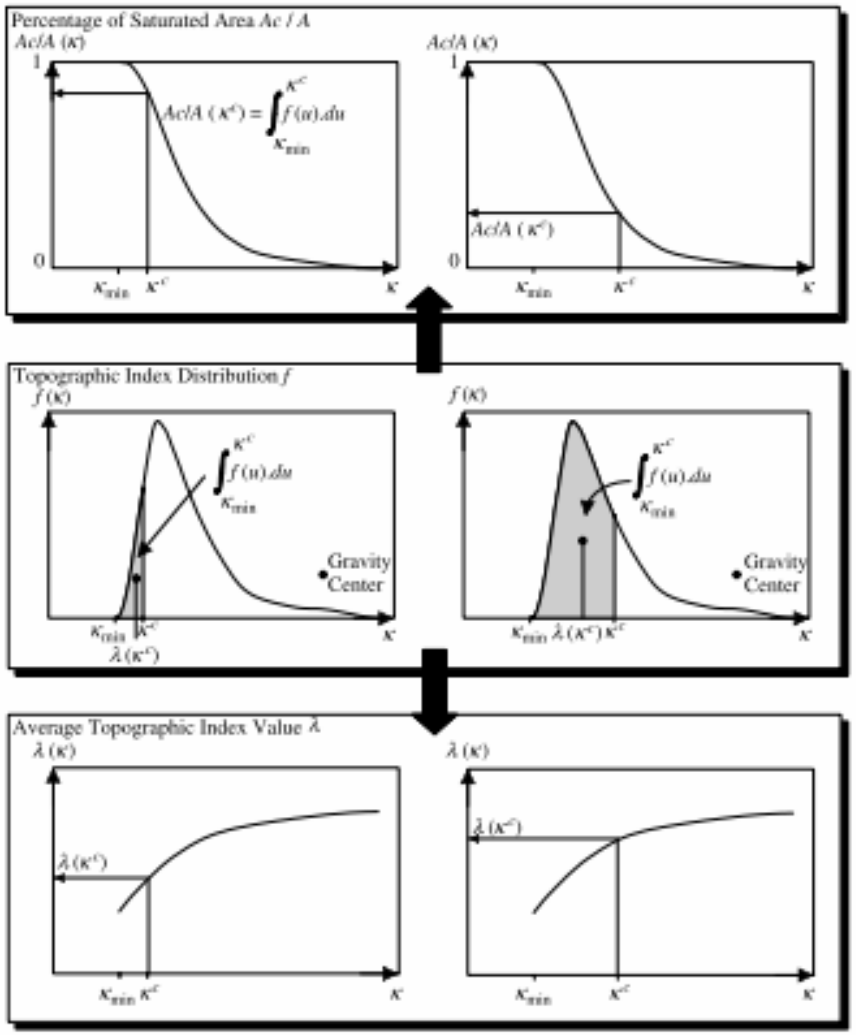

Figure 4. Terms of Equation (11) as a function of κ_t^c, the minimum value of the topographic index for soil saturation at time step t. A_{c_t}/A (a) is simply obtained by integration of the topographic index distribution (b), and λ_t^* (c) can be recognized as the abscissa of the gravity centre of the topographic index distribution truncated to values lower than or equal to κ_t^c

$$D_t^* - d_{i,t} = -m(\lambda_t^* - \kappa_i)$$

$$\lambda_t^* = \frac{1}{A - A_{c_t}} \int_{A-A_{c_t}} \ln\left(\frac{a_i}{T_o \tan\beta_i}\right) da$$

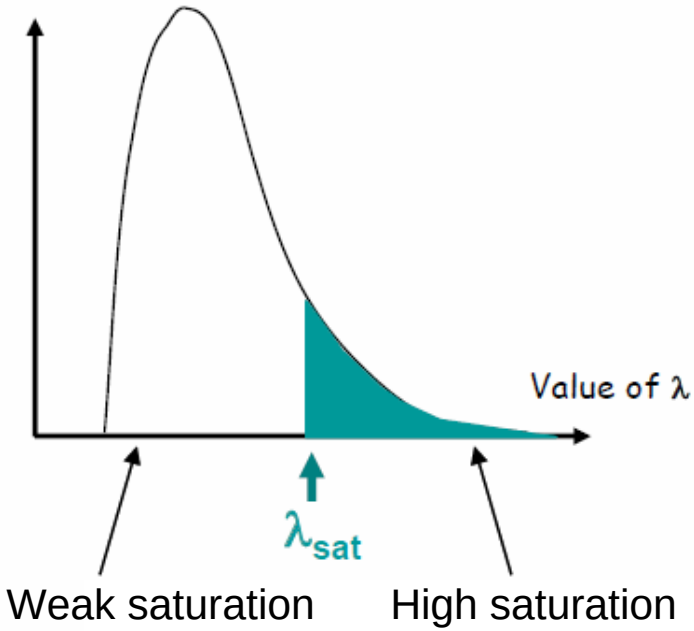

Saulnier and Datin, 2004

Simulated wetland extent

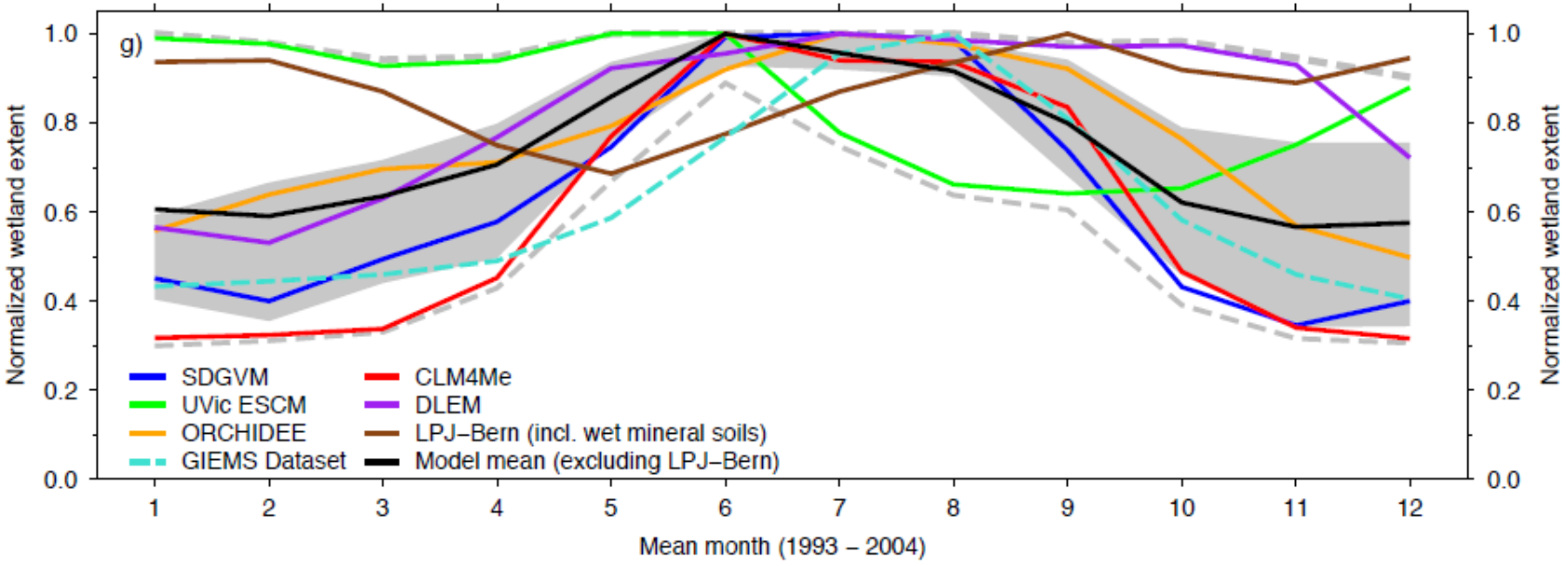

Melton et al., 2013

Satellites observed wetland extent

Prigent's 2007 dataset (GIEMS)

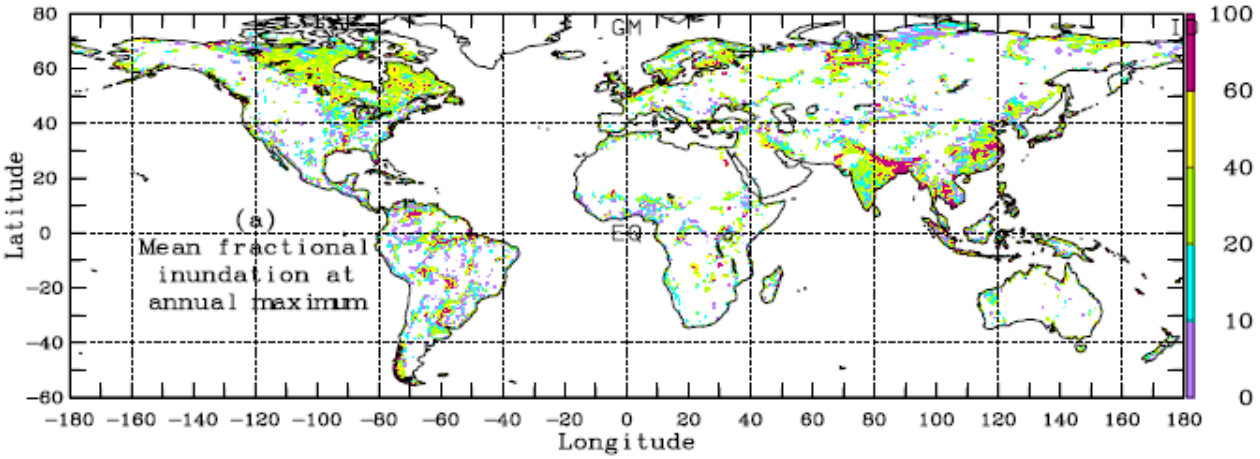

SWAMP

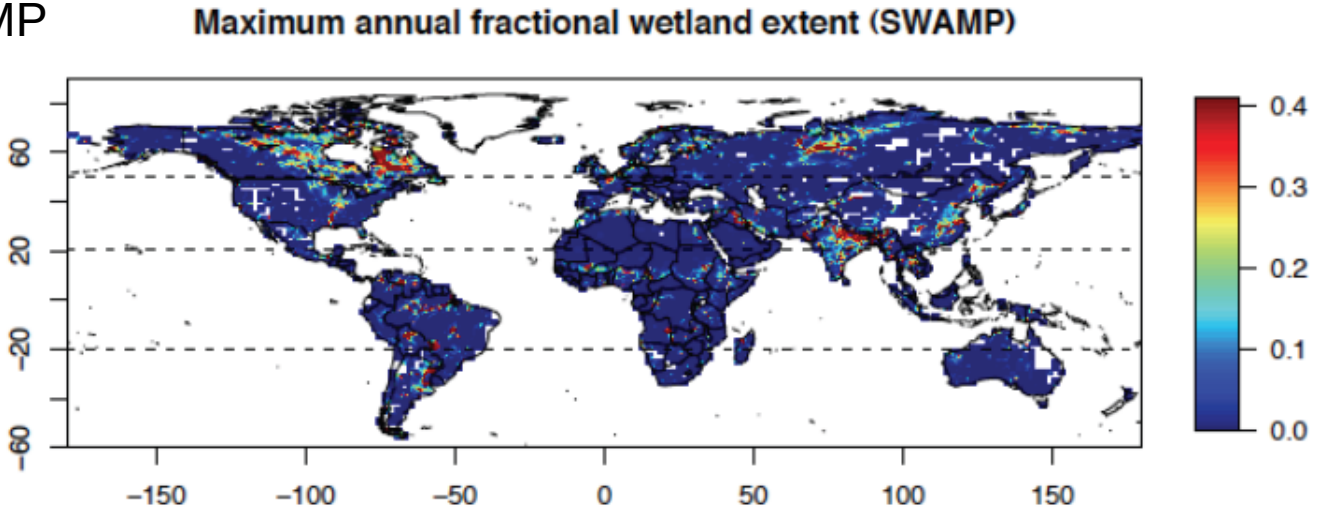

Simulated wetland extent

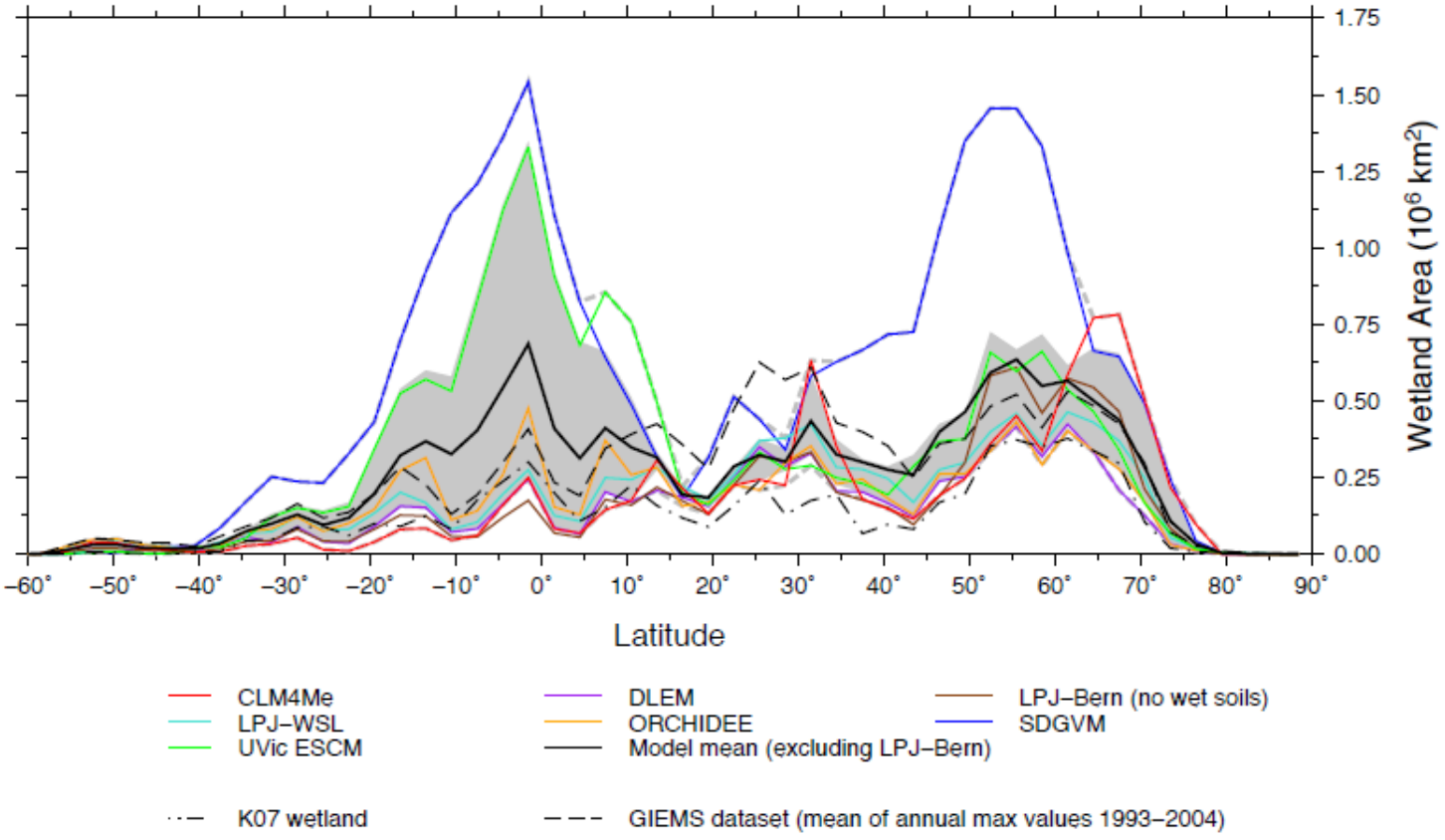

Melton et al., 2013

Simulated wetland methane emissions

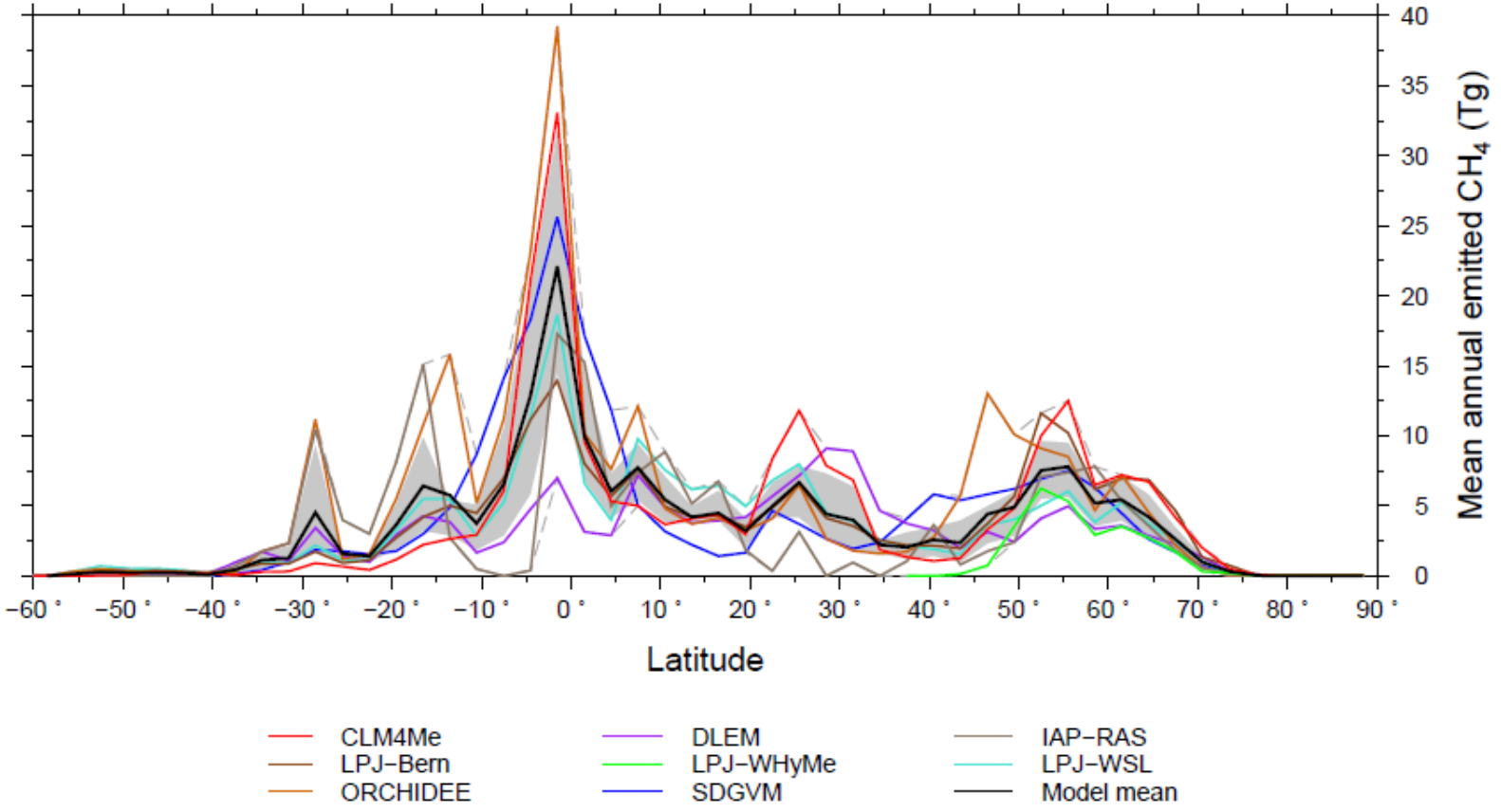

Melton et al., 2013

Simulated wetland methane emissions

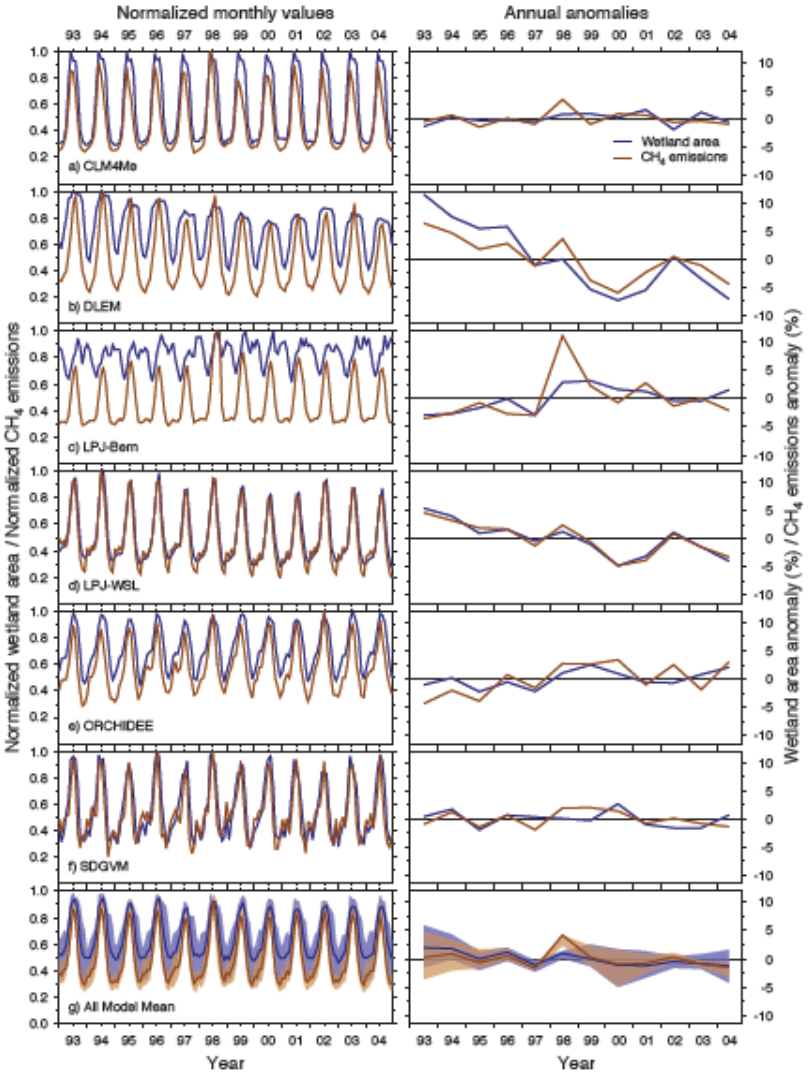

Wetland extent simulation is the key of wetland methane emissions.

Melton et al., 2013

Challenges

Hydrate from shelf, permafrost

Fugitive fossil fuel, shale gas

Boreal wetlands

Thermokarst lakes/ponds

Tropical wetlands

…

Methane clathrate

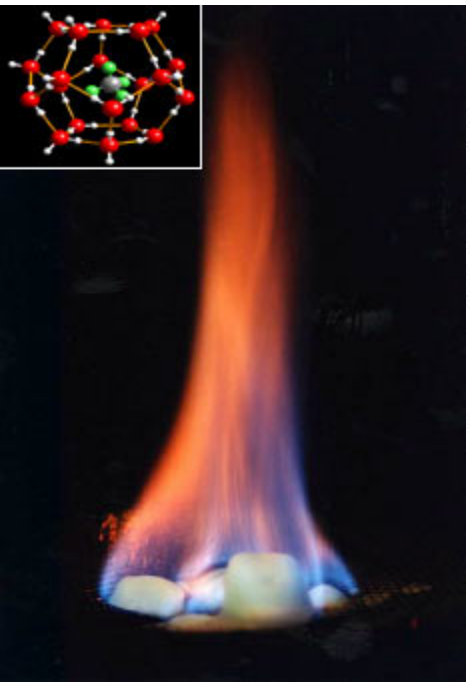

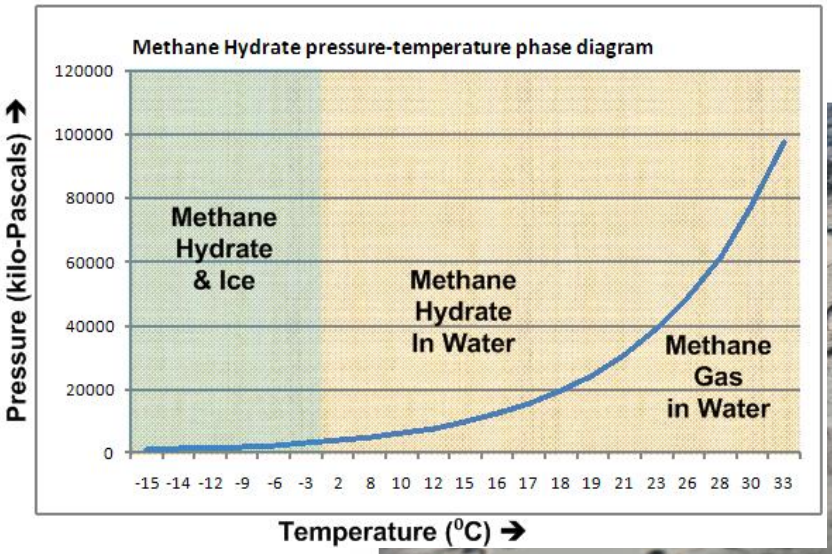

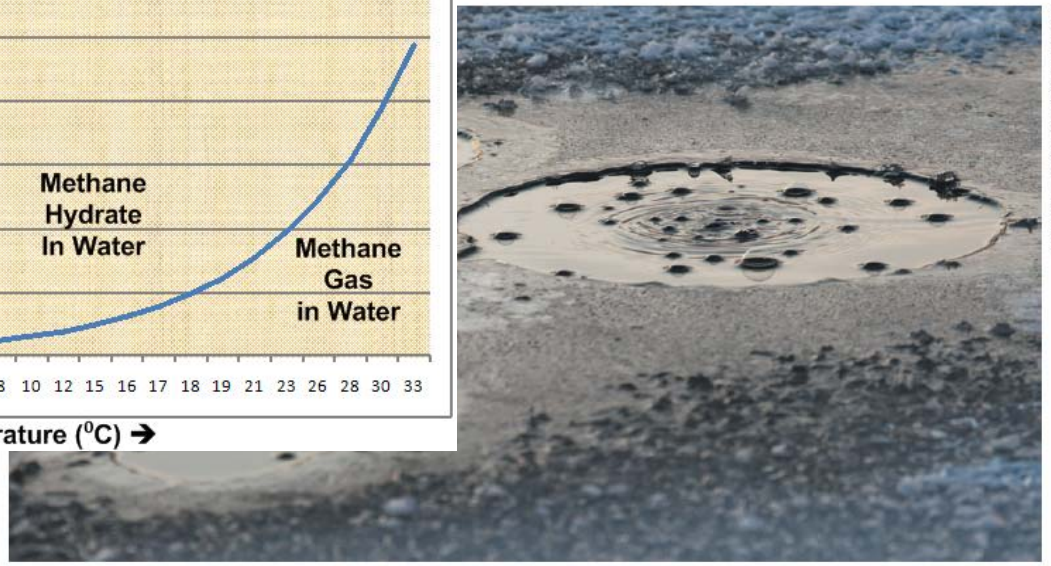

JOSH HANER/THE NEW YORK TIMES/REDUX/EYEVINE

Bubbles of methane emerge from sediments below a frozen Alaskan lake.

The Arctic is thought to be home to 30% of the world's undiscovered gas and 13% of its undiscovered oil, and new polar shipping

Whiteman et al., 2013, Nature

Fugitive methane from fossil fuel

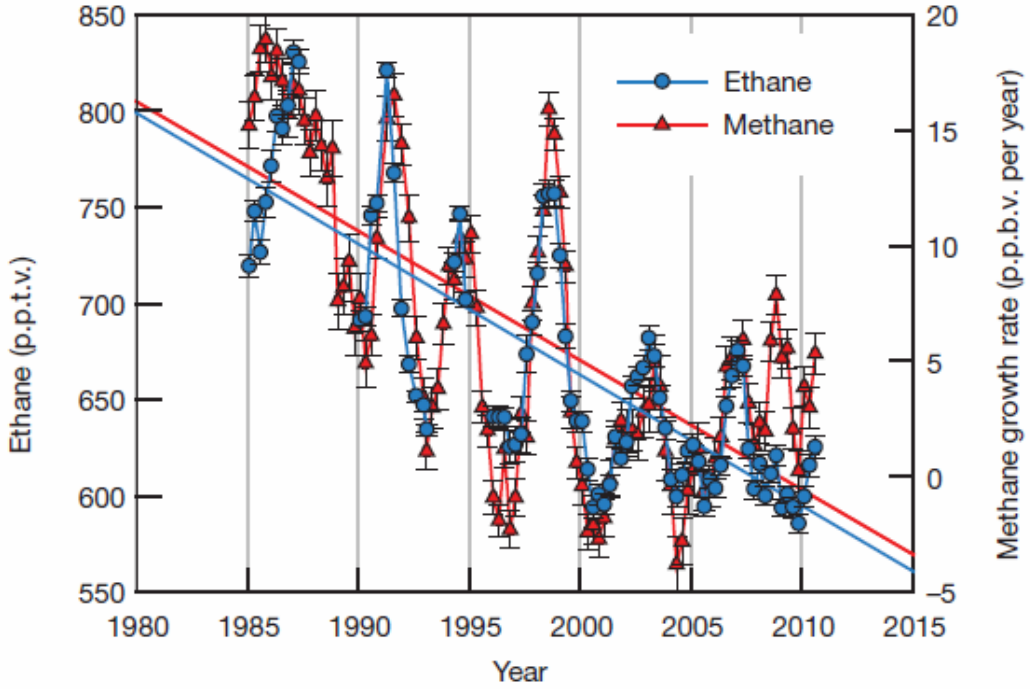

Figure 4 | Running global averages of ethane mixing ratios and methane growth rate. The methane measurements, which were co-sampled with

from 1984 to 2010. We attribute this to decreasing fugitive emissions from ethane's fossil fuel source—most probably decreased venting and flaring of natural gas in oil fields—rather than a decline in its other major sources, biofuel use and biomass burning. Ethane's major emission sources are shared with methane, and

Simpson et al., 2012

Boreal wetland

Increased precipitation

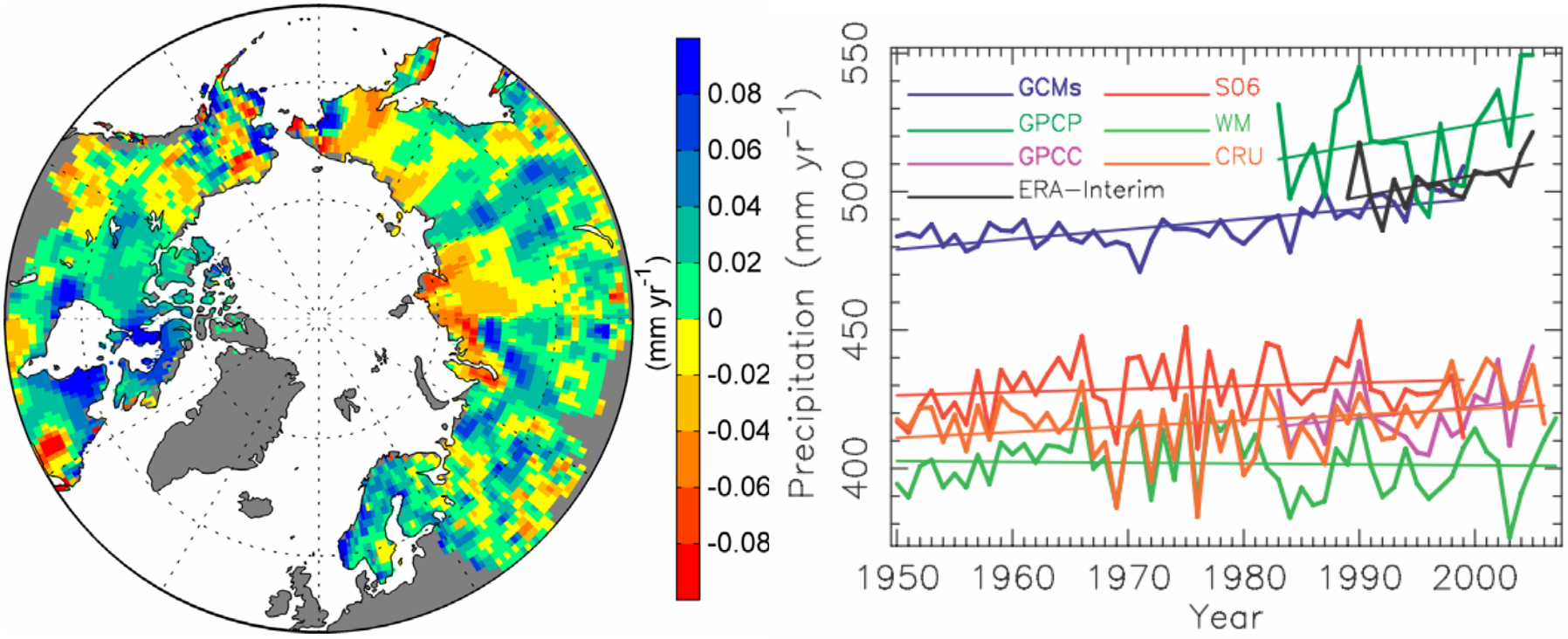

Rawlins et al., 2010

Thermokarst lakes

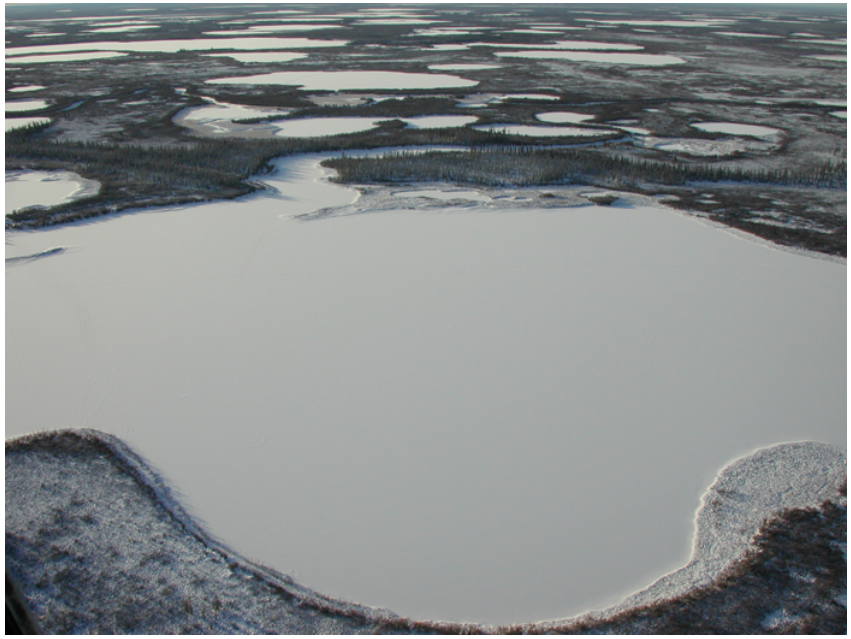

Source from Chen et al., 2013; WERC, UAF

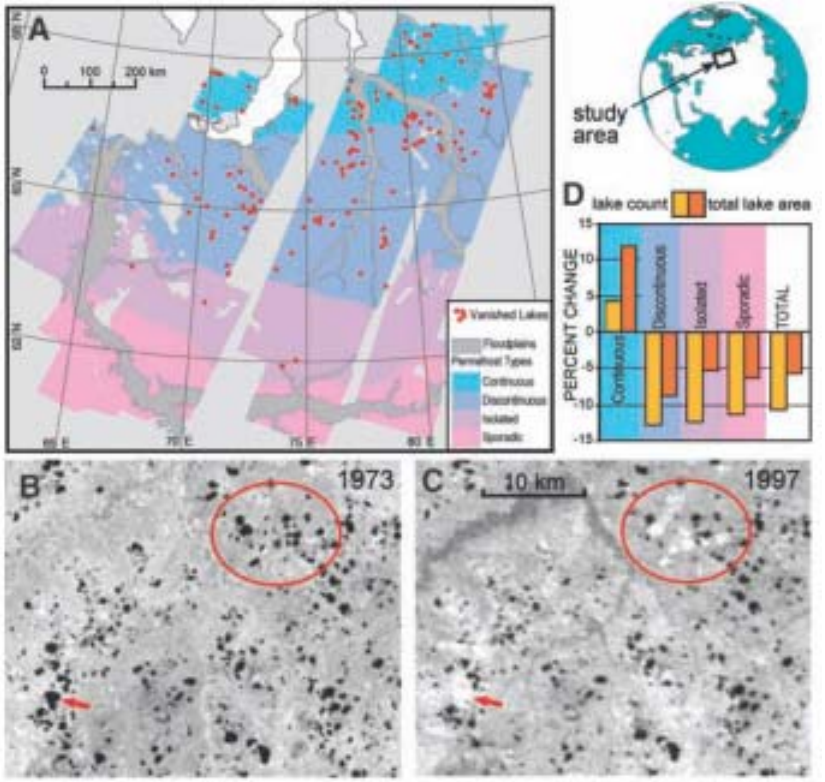

Fig. 1. (A) Locations of Siberian lake inventories, permafrost distribution, and vanished lakes. Total lake abundance and inundation area have declined since 1973 (B), including (C) permanent drainage and revegetation of former lakebeds (the arrow and oval show representative areas). (D) Net increases in lake abundance and area have occurred in continuous permafrost, suggesting an initial but transitory increase in surface ponding.

Smith et al., 2005, Science

Tropical wetlands

Changes in Precipitation

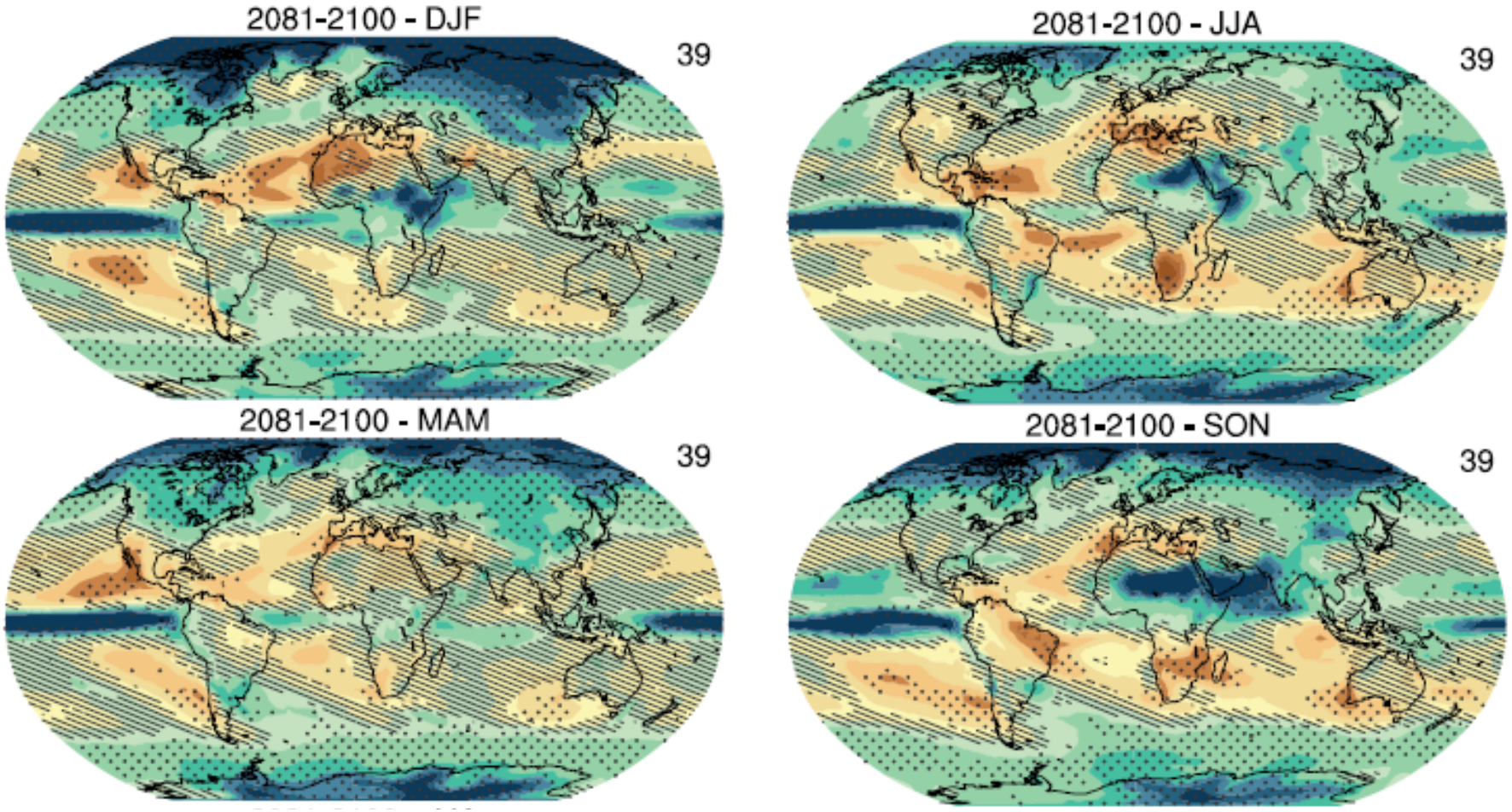

Tropical wetlands